UNCLASSIFIED

SECURITY CLASSIFICATION OF THIS PAGE

AD-A275 497

(2)

94-04282

REPORT DOCUMENTATION PAGE

1a. REPORT SECURITY CLASSIFICATION Unclassified

2a. SECURITY CLASSIFICATION AUTHORITY

2b. DECLASSIFICATION / DOWNGRADING SCHEDULE

3. DISTRIBUTION / AVAILABILITY OF REPORT
Approved for public release; distribution unlimited.

4. PERFORMING ORGANIZATION REPORT NUMBER(S)

5. MONITORING ORGANIZATION REPORT NUMBER(S)
ARO 27493.16-EL

6a. NAME OF PERFORMING ORGANIZATION
Dept. of Electrical and Computer Engineering
University of Massachusetts

6b. OFFICE SYMBOL *(If applicable)*

7a. NAME OF MONITORING ORGANIZATION
U. S. Army Research Office

6c. ADDRESS *(City, State, and ZIP Code)*
Marcus Hall
Box 35110
Amherst, MA 01003-5110

7b. ADDRESS *(City, State, and ZIP Code)*
P. O. Box 12211
Research Triangle Park, NC 27709-2211

8a. NAME OF FUNDING / SPONSORING ORGANIZATION
U. S. Army Research Office

8b. OFFICE SYMBOL *(If applicable)*

9. PROCUREMENT INSTRUMENT IDENTIFICATION NUMBER
DAAL03-91-G-0001

8c. ADDRESS *(City, State, and ZIP Code)*
P. O. Box 12211
Research Triangle Park, NC 27709-2211

10. SOURCE OF FUNDING NUMBERS

PROGRAM ELEMENT NO.	PROJECT NO.	TASK NO.	WORK UNIT ACCESSION NO

11. TITLE *(Include Security Classification)*
"Mean Acquisition Time for Noncoherent PN Sequence Sequential Acquisition Schemes" Unclassified.

12. PERSONAL AUTHOR(S) Lam, Alex W., Naval Postgraduate School, and Tantaratana, Sawasd

13a. TYPE OF REPORT

13b. TIME COVERED FROM ____ TO ____

14. DATE OF REPORT *(Year, Month, Day)*

15. PAGE COUNT

16. SUPPLEMENTARY NOTATION The view, opinions and/or findings contained in this report are those of the author(s) and should not be construed as an official Department of the Army position, policy, or decision, unless so designated by other documentation.

17. COSATI CODES

FIELD	GROUP	SUB-GROUP

18. SUBJECT TERMS *(Continue on reverse if necessary and identify by block number)*
Acquisition, PN acquisition, sequential acquisition, SPRT, spread spectrum, Noncoherent acquisition, DS/SS

19. ABSTRACT *(Continue on reverse if necessary and identify by block number)*

Sequential PN code acquisition schemes have the potential to achieve the best performance, but they are the least analyzed because of the analytical difficulties. In recent studies, we have proposed and investigated the truncated sequential probability ratio test (TSPRT) for spread-spectrum noncoherent PN code acquisition. It was shown to be much better than the conventional fixed sample size (FSS) scheme in the average sample number (ASN) at fixed detection and false-alarm probabilities. For system design purposes, however, the mean acquisition time is more informative. In this paper, we report results on the mean acquisition time for the TSPRT. Numerical data that includes Rician fading effect is also presented. Our results show that the proposed TSPRT is efficient, robust (against fading), fast, and suitable for real-time low-cost implementation.

94 2 08 010

20. DISTRIBUTION / AVAILABILITY OF ABSTRACT
☐ UNCLASSIFIED/UNLIMITED ☐ SAME AS RPT. ☐ DTIC USERS

21. ABSTRACT SECURITY CLASSIFICATION
Unclassified

22a. NAME OF RESPONSIBLE INDIVIDUAL

22b. TELEPHONE *(Include Area Code)*

22c. OFFICE SYMBOL

DD FORM 1473, 84 MAR — 83 APR edition may be used until exhausted. All other editions are obsolete.

SECURITY CLASSIFICATION OF THIS PAGE
UNCLASSIFIED

Mean Acquisition Time for Noncoherent PN Sequence Sequential Acquisition Schemes*

Alex W. Lam
Department of Electrical and Computer Engineering
Naval Postgraduate School, Monterey, CA 93943

Sawasd Tantaratana
Department of Electrical and Computer Engineering
University of Massachusetts, Amherst, MA 01003

ABSTRACT Sequential PN code acquisition schemes have the potential to achieve the best performance, but they are the least analyzed because of the analytical difficulties. In recent studies, we have proposed and investigated the truncated sequential probability ratio test (TSPRT) for spread-spectrum noncoherent PN code acquisition. It was shown to be much better than the conventional fixed sample size (FSS) scheme in the average sample number (ASN) at fixed detection and false-alarm probabilities. For system design purposes, however, the mean acquisition time is more informative. In this paper, we report results on the mean acquisition time for the TSPRT. Numerical data that includes Rician fading effect is also presented. Our results show that the proposed TSPRT is efficient, robust (against fading), fast, and suitable for real-time low-cost implementation.

1 Introduction

In direct-sequence spread-spectrum (DS/SS) systems, the receiver must align the locally generated pseudonoise (PN) code with the incoming PN code. This code synchronization process is usually performed in two steps: acquisition and tracking. First, the acquisition process coarsely aligns the phases of the two PN sequences to within one chip or a fraction of a chip. The tracking process then takes over and perform fine adjustment until the phase difference becomes ideally zero.

Extensive research on PN code acquisitions has been carried out during the past two decades [1]. In general, acquisition schemes can be classified into fixed-dwell, multiple-dwell, and sequential schemes. Sequential schemes have the potential to achieve the best performance, but they are the least studied because of the difficulty in design and analysis. In most reports on sequential schemes, the decision process is based on independent and identically distributed (i.i.d.) random variables. To obtain i.i.d. samples, the integrator in each correlation arm was reset periodically, which could reduce the effective signal-to-noise ratio. We use continuous integrations in our system.

Since the acquisition process involves searching through the uncertainty phases of the PN sequence, acquisition schemes can also be classified into parallel, serial, and hybrid schemes. A parallel scheme inspects all the uncertainty phases simultaneously and decides which is the most likely one. Each uncertainty phase is investigated by a path consisting of a correlator or a matched filter. If the period of the PN sequence is large, parallel schemes would require excessive hardware and, hence, are impractical. On the other hand, a serial scheme inspects one uncertainty phase at a time and determines whether the phase of the local sequence and the phase of the incoming sequence are in alignment. If they are, the tracking circuit is initiated. Otherwise, the next uncertainty phase is examined. Hardware requirements of such schemes are minimal, but the complexity of the control process increases. Various combinations of the serial search and the parallel search are possible.

We have studied the TSPRT and found that it was better than the FSS test in the ASN at fixed detection and false-alarm probabilities [2], [3], [4]. For system design purposes, the mean acquisition time is more suitable. In this paper, we report results on the mean acquisition time for the TSPRT.

*This work was supported by the Army Research Office under Grant No. DAAL03-91-G-0001. E-mail addresses: lam@ece.nps.navy.mil, tantaratana@ecs.umass.edu

2 System Model

The acquisition system under consideration is depicted in Figure 1. We assume that the channel has slowly-varying fading and additive white Gaussian noise with two-sided power spectral density $N_0/2$. We also assume that there is no data modulation during the acquisition process. The input signal at the receiver is

$$r(t) = A_0\psi a(t + i\Delta T_c)\cos(\omega_0 t + \theta) \; + \; n(t) \tag{1}$$

where A_0 is the signal amplitude, $a(t)$ is the PN waveform, ψ is the fading random variable, i is an integral phase number, Δ is a value determining how much the timing of the local PN generator is updated during the search process, T_c is the chip duration, ω_0 and θ are the frequency and phase of the carrier, and $n(t)$ is the additive noise. If there is no fading, $\psi = 1$ with probability 1. The value of Δ is usually 1 or 1/2, meaning that the local phase is updated each time by T_c or $T_c/2$.

The fading is assumed to be Rician, i.e., ψ has a Rician probability density function (pdf) given by

$$f_\psi(\psi) = 2\psi(1+r)e^{-r-\psi^2(1+r)}I_0\left(2\psi\sqrt{r(1+r)}\right), \psi \geq 0, \tag{2}$$

where r is the ratio of the power in the direct component (s^2) and the power in the diffused component ($2\sigma^2$), i.e., $r = s^2/(2\sigma^2)$, with the constraint that $s^2 + 2\sigma^2 = 1$. Note that $s^2 = r/(1+r)$ and $\sigma^2 = 0.5/(1+r)$. When $r = \infty$ (or $\sigma^2 = 0$ and $s^2 = 1$), it corresponds to no fading. When $r = 0$ (or $s^2 = 0$ and $\sigma^2 = 0.5$), we have Rayleigh fading, for which case the pdf of ψ is given by $f_\psi(\psi) = 2\psi e^{-\psi^2}$, $\psi \geq 0$.

Let the locally generated PN waveform be $a(t + (j + \gamma)\Delta T_c)$, where j is an integer and $|\gamma| < 1/2$. The received signal $r(t)$ is first multiplied by the local PN waveform and then noncoherently demodulated (see Figure 1). The result Y_n is used by the decision processor to test if the local and the incoming PN waveforms are aligned to within $\Delta T_c/2$ seconds. When (coarse) alignment is achieved, we have $j = i$ and the tracking circuit is initiated to bring γ to zero.

0-7803-0953-7/93$03.00

Otherwise, the phase of the local PN waveform is updated by ΔT_c seconds and the acquisition process continues.

Referring to Figure 1, we see that the decision statistic, y_n, is compared to some threshold values. In the case of TSPRT, the test will be truncated at some time instance $n = n_0$. For time instance $1 \leq n \leq n_0$, y_n is compared to two thresholds, $A(n)$ and $B(n)$, where $A(n) > B(n)$. If $y_n \geq A(n)$, then the processor will decide that PN code acquisition is achieved and the PN code tracking loop will be activated. If $y_n \leq B(n)$, then a non-synchronization situation will be decided; the local PN code timing will be updated by ΔT_c seconds, the integrators are reset, and a new test run is initiated. If y_n is between $A(n)$ and $B(n)$, no decision will be made at time instance n; one more chip duration will be integrated and the test continues for the next value of n. If no decision has been made at time instance $n = n_0 - 1$, the test is terminated at $n = n_C$. In this case, y_{n_0} is compared to one single threshold $\hat{r}'$ and a synchronization decision is favored if $y_{n_0} > \hat{r}'$, otherwise, a non-synchronization decision is favored if $y_{n_0} < \hat{r}'$. The designs of the truncation time n_0, thresholds $\hat{r}'$, $A(n)$ and $B(n)$ have been discussed in details in [2], [3], and [4] for fading as well as non-fading channels. In Figure 2 we show a typical threshold design for the TSPRT.

3 Mean Acquisition Time

It was found in [2] that for fixed false-alarm and detection probabilities, a properly designed TSPRT is superior to the FSS test in the average sample number (ASN). For system design purposes, the mean acquisition time, which is the average time for a test to achieve code acquisition, is a more desirable performance measure. In this paper, we present results on the mean acquisition time for the TSPRT.

In a serial search acquisition scheme, such as the TSPRT, the mean acquisition time can be readily obtained using the flow-graph technique [5], [6]. We show a circular flow-graph diagram for TSPRT in Figure 3(a). This flow-graph has a total of $\nu + 2$ states. Two of these states are the acquisition state and the false-alarm state, where the former is absorbing and the latter is not. The remaining $\nu = N/\Delta$ states are searching states, where N is the PN code sequence period and Δ (taken to be 1/2 in this paper) is the fraction of a chip to be updated each time a non-synchronization decision is made. We assume that the code tracking loop following the acquisition circuit can successfully track the incoming code phase if the phase offset is smaller than T_c seconds. If we set $\gamma = 1/2$, where γT_c is the timing difference between the incoming and the locally generated PN waveforms when $j = i$, then a total of four states will correspond to H_1 (alignment hypothesis), i.e., state $\nu - 1$, ν, 1, and 2, as shown in Figure 3(a); the corresponding detection probabilities and ASN's can be evaluated [2]. In this paper, the prior probabilities, p_i's, are assumed to be uniformly distributed. Because a false-alarm decision will be costly, a verification mode is also incorporated in the scheme [5], where A or less additional tests are performed before making a final decision. The initial decision will hold if B ($\leq A$) additional tests are favorable; otherwise, it is overturned and the search continues for the next searching state. In this paper, we assume that a counter is available and the coincidence detector (CD) employs an early termination mechanism in order to save time. In particular, the CD will terminate testing once B favorable tests are accumulated or when there is no chance that B favorable tests can be obtained. Figure 4 describes the coincidence detection process in detail.

We are interested in finding the gain function $P_{acq}(z)$, where

$$P_{acq}(z) = \sum_{i=1}^{\nu} p_i P_{i,acq}(z) \tag{3}$$

with $P_{i,acq}(z)$ denoting the gain function going from state i to the acquisition state ACQ and $p_i = 1/\nu = 1/2N$. Contrary to the typical flow-graph diagrams discussed in [5] and [6], our gain functions for the H_0 (non-alignment) states are not identical. More importantly, the time delays, t_j's are random variables instead of constants. We also do not lump the four H_1 states into one single state, and our model in Figure 3(a) describes the serial acquisition process more satisfactorily. Inspecting the flow-graph diagram, we can obtain:

$$\begin{aligned} P_{\nu-1,acq}(z) &= [(D_{\nu-1} + M_{\nu-1}D_\nu + M_{\nu-1}M_\nu D_1 \\ &\quad + M_{\nu-1}M_\nu M_1 D_2)(z)]/[1 - M_1 \cdots M_\nu(z)] \end{aligned}$$

$$\begin{aligned} P_{\nu,acq}(z) &= [(D_\nu + M_\nu D_1 + M_\nu M_1 D_2 + M_\nu M_1 \cdots \\ &\quad \cdot\cdot M_{\nu-2}D_{\nu-1})(z)]/[1 - M_1 \cdots M_\nu(z)] \end{aligned}$$

$$\begin{aligned} P_{1,acq}(z) &= [(D_1 + M_1 D_2 + M_1 M_2 \cdots M_{\nu-2}D_{\nu-1} \\ &\quad + M_1 \cdots M_{\nu-1}D_\nu)(z)]/[1 - M_1 \cdots M_\nu(z)] \end{aligned}$$

$$\begin{aligned} P_{2,acq}(z) = [(D_2 + M_2 \cdots M_{\nu-2}D_{\nu-1} + M_2 \cdots M_{\nu-1}D_\nu \\ + M_2 \cdots M_\nu D_1)(z)]/[1 - M_1 \cdots M_\nu(z)] \end{aligned} \tag{4}$$

Here, $M(z)$ stands for the *miss* gain function and $D(z)$ the *detection* gain function. The above four expressions are the gain functions for the four states under H_1. In particular, state $\nu - 1$ corresponds to the situation when $j + \gamma = -1.5$, state ν for $j + \gamma = -0.5$, state 1 for $j + \gamma = 0.5$, and state 2 for $j + \gamma = 1.5$. All the other searching states are under H_0, with gain functions given by:

$$\begin{aligned} P_{3,acq}(z) &= M_3 M_4 \cdots M_{\nu-2} P_{\nu-1,acq}(z) \\ P_{4,acq}(z) &= M_4 M_5 \cdots M_{\nu-2} P_{\nu-1,acq}(z) \\ &\cdots \\ &\cdots \\ P_{\nu-2,acq}(z) &= M_{\nu-2} P_{\nu-1,acq}(z) \end{aligned} \tag{5}$$

These equations can be easily derived from the flow-graph diagram. Next, we can find the individual gain functions as follows:

$$\begin{aligned} M_{\nu-1}(z) &= (1 - P_d(\nu-1))z^{t_{\nu-1}} \\ &\quad + P_d(\nu-1)(1 - P_{cd}(\nu-1))z^{t_{\nu-1}+t'_{\nu-1}} \\ D_{\nu-1}(z) &= P_d(\nu-1)P_{cd}(\nu-1)z^{t_{\nu-1}+t'_{\nu-1}} \end{aligned} \tag{6}$$

where $P_d(\nu - 1)$ is the *detection* probability and $P_{cd}(\nu - 1)$ the *coincidence* detector detection probability for state $\nu - 1$. The time delay $t'_{\nu-1}$ is a sum of A or less delay terms. Based on the early-termination coincidence detection process described in Figure 4, we may model the coincidence detection probability $P_{cd}(\nu - 1)$ and the time delay $t'_{\nu-1}$ respectively as:

$$\begin{aligned} P_{cd}(\nu-1) &= \sum_{j=0}^{A-B} \frac{(A-j-1)!}{(B-1)!(A-j-B)!} \\ &\quad \cdot (1 - P_d(\nu-1))^{A-j-B}(P_d(\nu-1))^B \end{aligned} \tag{7}$$

and

$$t'_{\nu-1} = \sum_{j=0}^{A-B} \frac{(A-j-1)!}{(B-1)!(A-j-B)!}(1-P_d(\nu-1))^{A-j-B} \cdot (P_d(\nu-1))^B (A-j)\cdot t_{\nu-1} + \sum_{j=0}^{B-1} \frac{(A-B+j)!}{j!(A-B)!}(1-P_d(\nu-1))^{A-B+1} \cdot (P_d(\nu-1))^j (A-B+1+j)\cdot t_{\nu-1} \quad (8)$$

Referring to Figure 4, we note that the coincidence detection probability can also be written as

$$P_{cd}(\nu-1) = 1-\sum_{j=0}^{B-1} \frac{(A-B+j)!}{j!(A-B)!}(1-P_d(\nu-1))^{A-B+1} \cdot (P_d(\nu-1))^j \quad (9)$$

We remark that the coincidence tests are statistically independent. The early termination procedure saves time, but it would not affect the coincidence detection probability, which is also equal to

$$P_{cd}(\nu-1) = \sum_{j=B}^{A} \frac{A!}{j!(A-j)!}(1-P_d(\nu-1))^{A-j}(P_d(\nu-1))^j \quad (10)$$

The equivalence of equations (7), (9) and (10) can be verified by combinatorial arguments. With a straightforward substitution of indices in the above expressions, $M_\nu(z), D_\nu(z), M_1(z), D_1(z), M_2(z)$, and $D_2(z)$ can be found similarly. For the false-alarm states, we can write

$$M_3(z) = NFA_3(z) + FA_3(z)\cdot R_3(z) \quad (11)$$

where

$$NFA_3(z) = (1-P_{fa}(3))z^{t_3} + P_{fa}(3)(1-P_{cfa}(3))z^{t_3+t'_3}$$
$$FA_3(z) = P_{fa}(3)P_{cfa}(3)z^{t_3+t'_3}$$
$$R_3(z) = z^{cNT_c} \quad (12)$$

In the above equation, $FA_3(z)$ and $NFA_3(z)$ are the gain functions for the false-alarm and correct dismissal, respectively, and $R_3(z)$ is the return gain function for state 3, which specify the penalty time incurred in returning from the false-alarm (FA) state. The constant c is the number of bit intervals elapsed before returning from the FA state. Note that we have assumed that one bit duration is exactly one period of the PN code, which has N chips. Also note that $P_{fa}(3)$ denotes the false-alarm probability, and $P_{cfa}(3)$ the coincidence false-alarm probability, for state 3. The gain functions for states $4, 5, \cdots, \nu-2$ are similar. The coincidence false-alarm probabilities and time delays for these H_0 states can be evaluated using equations (7) and (8) by substituting P_d with P_{fa}.

The overall acquisition probability is given by $P_{acq}(1)$, which is equal to 1 because the ACQ state is the only absorbing state in this case. The mean acquisition time, conditioning on all the time delays, is equal to the differentiation of $P_{acq}(z)$ (with respect to z) evaluated at $z=1$. Towards this end, we see that

$$P'_{\nu-1,acq}(1) = [D'_{\nu-1}(1) + (M_{\nu-1}D_\nu)'(1) + (M_{\nu-1}M_\nu D_1)'(1) + (M_{\nu-1}M_\nu M_1 D_2)'(1)] \cdot [1-(M_1M_2M_3\cdots M_\nu)(1)]^{-1} + [D_{\nu-1}(1) + M_{\nu-1}D_\nu(1) + (M_{\nu-1}M_\nu D_1)(1) + (M_{\nu-1}M_\nu M_1 D_2)(1)]\cdot[(M_1M_2M_3\cdots M_\nu)'(1)] \cdot [1-(M_1M_2M_3\cdots M_\nu)(1)]^{-2} \quad (13)$$

where

$$M'_{\nu-1}(1) = (1-P_d(\nu-1))t_{\nu-1} + P_d(\nu-1)(1-P_{cd}(\nu-1))(t_{\nu-1}+t'_{\nu-1}) \quad (14)$$

and

$$D'_{\nu-1}(1) = P_d(\nu-1)P_{cd}(\nu-1)(t_{\nu-1}+t'_{\nu-1}) \quad (15)$$

The differentiation of a product of terms is made easy by using the chain rule:

$$(\prod_k f_k(x))' = \prod_k f_k(x)\cdot\sum_k \frac{f'_k(x)}{f_k(x)} \quad (16)$$

One can see that $M_i(1)$ and $D_i(1)$ are constants, and each $P'_{i,acq}(1)$ is a linear function of the time delays t_i and t'_i. Thus, by replacing the time delays by their expected values, we can compute the mean acquisition time, $E(T_{acq})$, where

$$E(T_{acq}) = P'_{acq}(1) = \sum_{i=1}^{\nu} p_i P'_{i,acq}(1) \quad (17)$$

We note that

$$\begin{aligned} E(t_{\nu-1}) &= ASN_{-1.5}\cdot T_c = ASN_{1.5}\cdot T_c \\ E(t_\nu) &= ASN_{-0.5}\cdot T_c = ASN_{0.5}\cdot T_c \\ E(t_1) &= ASN_{0.5}\cdot T_c \\ E(t_2) &= ASN_{1.5}\cdot T_c \\ E(t_3) &= E(t_4) = \cdots = E(t_{\nu-2}) \\ &= ASN_{2.5}\cdot T_c = ASN_2\cdot T_c \end{aligned} \quad (18)$$

and

$$E(t'_i) = c_i\cdot E(t_i) \quad (19)$$

for each i, and where c_i is known constant (see equation (8)). The values of $ASN_{1.5}$, $ASN_{0.5}$, and ASN_2, plus all the detection and false alarm probabilities can be evaluated using techniques described in [2].

4 Numerical Results and Discussions

In this section we present results for the TSPRT with chip $SNR = A_0^2T_c/2N_o = -10$dB and PN code sequence period $N = 1023$.

First, we set the design probabilities to be $P_d = 0.99$ (at H_1) and $P_{fa} = 0.01$ (at H_0). The ASN values and the power of the TSPRT were displayed in Table 1 for $r = \infty$ (no fading), $r = 10$, and $r = 0$ (Rayleigh fading). The TSPRT designed under our rules actually achieved a better detection probability (= 0.9921) than the desirable value (= 0.99) for $r = \infty$. Note that fading reduced $P_d(\nu)$, the detection probability, but it did not affect the ASN values significantly. We have considered different coincidence detector designs of (A, B). The number A is the maximum number of additional coincidence tests to be performed before committing an acquisition decision and B is the number of favorable tests required. For each A, there is an optimum choice of B^*. We computed several cases and evaluated the normalized mean acquisition time, $E(T_{acq})/T$, in units of number of bit intervals. The results were displyed in Table 2. For example, when $A = 5$ without early termination, we found that $B^* = 3$, $E(T_{acq})/T = 166.5$ bits for $r = \infty$ (no fading); likewise, when $A = 3$ with early termination, we have $B^* = 2$, $E(T_{acq})/T = 160.2$ bits for $r = 10$ (moderate fading).

Next, we tried different design probabilities and set $P_d = 0.9$ (at H_1) and $P_{fa} = 0.1$ (at H_0). Only the no fading case was considered and the corresponding numerical results were also included in Tables 1 and 2. To better understand the searching algorithm, we computed the individual time for the TSPRT to reach the acquisition state ARQ from each of the $2N$ states in the flow-graph. In our model, the states $\nu - 1$, ν, 1, 2 correspond to H_1, while all the other states 3, 4, ... , $\nu - 2$ correspond to H_0. One can show that for various typical coincidence detection scenarios, the time to reach ACQ from one of the four H_1 states are relatively small, which was in the order of 10 bit intervals or less in these examples. Furthermore, one can also show that the time to acquire is the smallest when the start state is at $\nu - 1$ or ν, and that it is maximum at start state 3 ($\approx$ 200 bits in these examples) and decreasing afterwards. For systems with small P_{fa}, the mean acquisition time is roughly approximated by ASN_2 bits. We stress the important point that the time to acquire under H_0 bears far much more weight than that would under H_1. Our results suggest that the H_0 state should be the major design consideration and $P'_{3,acq}(1)$ is an excellent parameter to optimize.

We conclude this paper as follows: (1) It pays to employ the coincidence detector since the mean acquisition time can be greatly reduced. (2) The design of the coincidence detector depends on various system parameters and there is no simple rule; however, using $(A, B) = (1, 1)$, or $(2, 1)$, or $(2, 2)$ suffices for a simple yet suboptimal design. (3) The TSPRT is quite robust against fading in tems of its mean acquisition time performance.

References

[1] M. K. Simon, J. K. Omura, R. A. Scholtz, and B. K. Levitt, *Spread Spectrum Communications*, Volume III, Maryland: Computer Science Press, 1985.

[2] S. Tantaratana, A. W. Lam, and P. Vincent, "Noncoherent sequential acquisition of PN sequences for DS/SS communications with/without fading," submitted to the *IEEE Trans. Commun.*

[3] S. Tantaratana and A. W. Lam, "Noncoherent sequential acquisition of PN sequences for DS/SS communications," *Proceedings of the Twenty-Ninth Allerton Conference on Communications, Control, and Computing*, University of Illinois, pp. 370-379, Oct. 1991.

[4] A. W. Lam, S. Tantaratana, and P. Vincent, "Effects of fading and modulation on sequential PN acquisitions in DS/SS communications," *Proceedings IEEE Military Communications Conferences*, pp. 17.1.1 – 17.1.5, San Diego, Oct. 1992.

[5] A. Polydoros and C. L. Weber, "A unified approach to serial search spread-spectrum code acquisition - Part I: general theory," *IEEE Trans. Commun.*, Vol COM-32, pp. 542 – 549, May 1984.

[6] A. Polydoros and C. L. Weber, "A unified approach to serial search spread-spectrum code acquisition - Part II: a matched-filter receiver," *IEEE Trans. Commun.*, Vol. COM-32, pp. 550 – 560, May 1984.

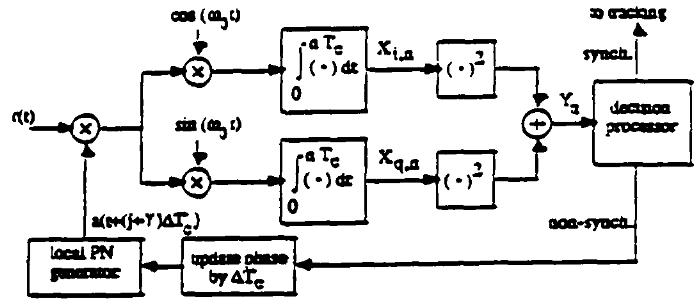

Figure 1: Block diagram of noncoherent serial acquisition scheme.

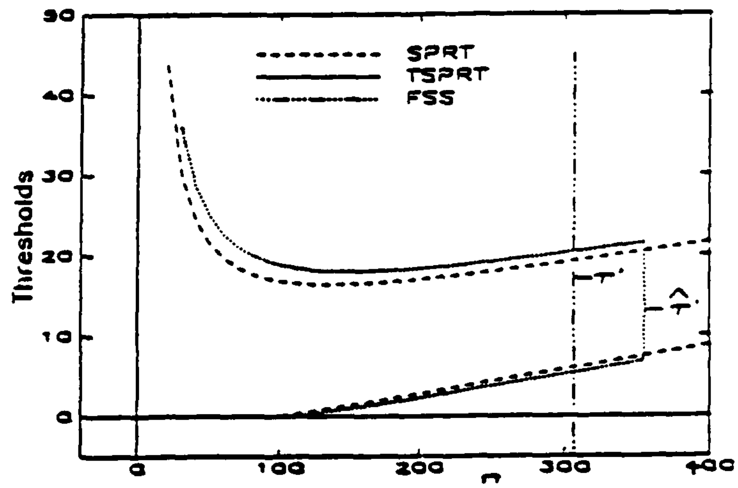

Figure 2: Thresholds for the test in Figure 1.

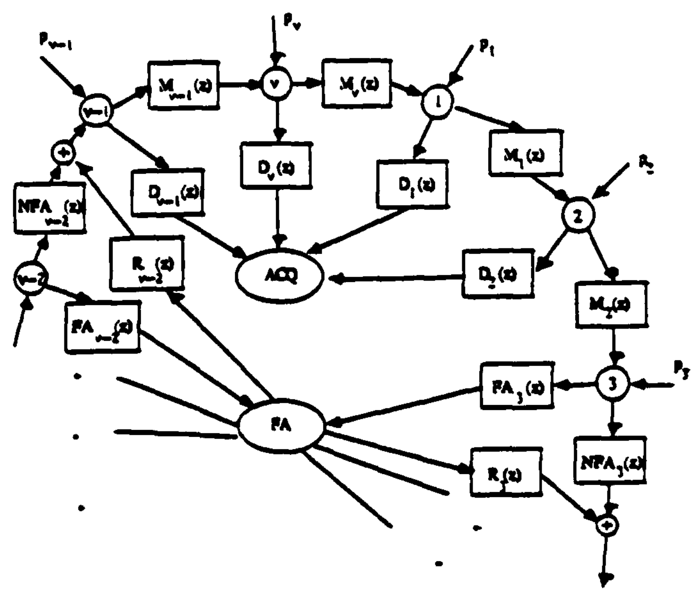

(a)

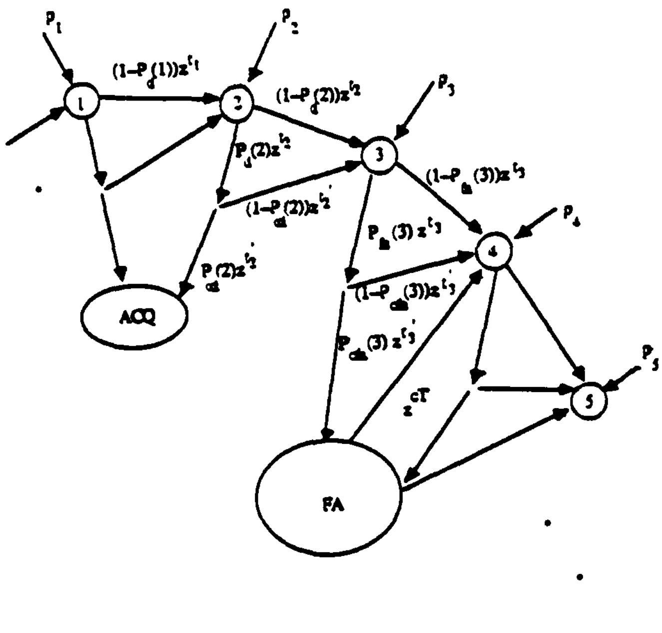

(b)

Figure 3: Circular flow-graph diagram for TSPRT. (a) general (b) detailed.

	$P_d = 0.99$, $P_{fa} = 0.01$			$P_d = 0.9$, $P_{fa} = 0.1$
	$r = \infty$	$r = 10$	$r = 0$	$r = \infty$
$ASN_{1.5}$	196.3	193.8	187.8	97.9
$ASN_{0.5}$	137.8	148.8	158.5	80.6
ASN_2	157.8	155.3	155.4	90.0
$P_d(v-1)$	.1157	.1253	.1464	.2049
$P_d(v)$	.9921	.9296	.7241	.9373
$P_d(1)$	.9921	.9296	.7241	.9373
$P_d(2)$	.1157	.1253	.1464	.2049
$P_{fa}(3)$	.0100	.0074	.0088	.0677

Table 1: TSPRT specifications.

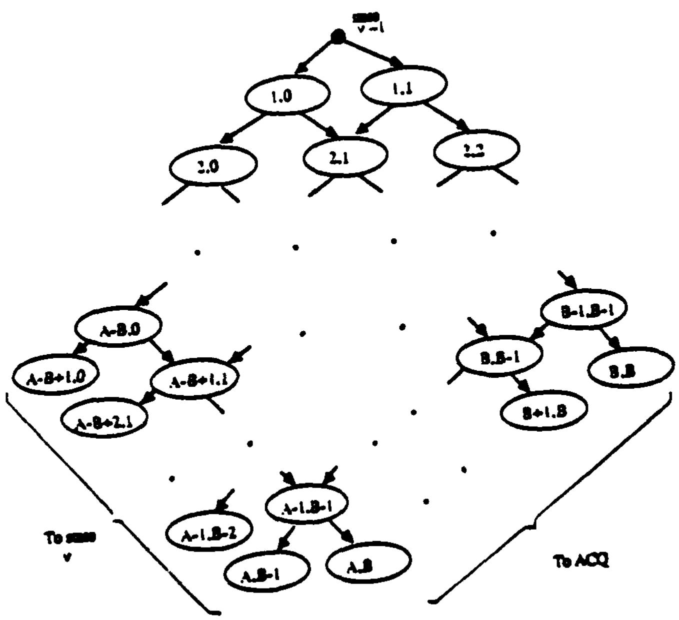

Figure 4: Coincidence detection with early termination.

	$P_d = 0.99$ $P_{fa} = 0.01$						$P_d = 0.9$ $P_{fa} = 0.1$	
	no termination			with termination			no term.	with term.
B^*, $E(T_{acq})/T$	$r = \infty$	$r = 10$	$r = 0$	$r = \infty$	$r = 10$	$r = 0$	$r = \infty$	$r = \infty$
A = 0	0, 208.8	0, 194.3	0, 224.0	0, 208.8	0, 194.3	0, 224.0	0, 437.3	0, 437.3
A = 1	1, 160.1	1, 162.6	1, 244.4	1, 160.1	1, 162.6	1, 244.4	1, 122.8	1, 122.8
A = 2	2, 161.4	1, 160.1	1, 195.0	2, 159.8	1, 160.0	1, 194.9	2, 110.5	2, 104.4
A = 3	2, 163.0	2, 161.5	1, 187.5	3, 160.1	2, 160.2	1, 187.2	2, 114.2	3, 107.5
A = 4	3, 164.7	2, 162.2	1, 186.9	4, 160.4	2, 160.8	1, 186.4	3, 116.6	3, 105.1
A = 5	3, 166.5	2, 163.4	1, 187.9	5, 160.8	3, 161.0	1, 187.2	3, 122.8	4, 105.3
A = 6	3, 168.2	2, 164.7	1, 189.4	6, 161.2	4, 161.3	1, 188.5	4, 128.2	5, 106.0
A = 7	3, 169.9	2, 166.0	1, 191.0	7, 161.6	5, 161.6	2, 189.4	4, 134.4	6, 106.9
A = 8	3, 171.6	2, 167.3	1, 192.8	8, 162.0	6, 162.1	2, 190.3	5, 140.5	7, 108.0

Table 2: Mean acquisition time for TSPRT.